MORPHOLOGIC CHARACTERISTICS AND EROSIVE RESISTANCE OF FELSIC ALKALINE INTRUSIVE MASSIF OF TANGUÁ, STATE OF RIO DE JANEIRO, BRAZIL, BASED ON THE ASTER GDEM

Akihisa MOTOKI [1], Susanna Eleonora SICHEL [2]; Samuel da SILVA [2], Kenji Freire MOTOKI [2]

(1) Departamento de Mineralogia e Petrologia Ígnea, Universidade do Estado do Rio de Janeiro (DMPI/UERJ). Rua São Francisco Xavier 524, Sala A-4023, Maracanã, Rio de Janeiro, CEP 20550-900, RJ. Endereço eletrônico: motokiakihisa@gmail.com.
(2) Departamento de Geologia, Universidade Federal Fluminense (DG/UFF). Av. General Milton Tavares de Souza s/n, 4º andar, Gragoatá, Niterói, CEP. 24210-340, RJ. Endereço eletrônico: susanna@id.uff.br, samueltec@gmail.com, kenji_dl@hotmail.com.

Introduction
Research Methods
Tanguá felsic alkaline intrusive body
Summit level maps
Base level maps and relief amount maps
Macro concavity index
Drainage system
Altitude distribution histogram
Landform origin
Conclusion
Acknowledgement
Reference

RESUMO - *Motoki, A. Sichel, S.E., Silva, S., Motoki, K.F. Características morfológicas e resistência erosiva do maciço intrusivo de rochas alcalinas félsicas de Tanguá, RJ, com base no ASTER GDEM.* Este artigo apresenta características morfológicas e resistência erosiva do maciço intrusivo de rochas alcalinas félsicas de Tanguá, RJ, com base nos dados topográficas de satélite do ASTER GDEM. O maciço intrusivo possui uma extensão de 5.5 x 7.5 km e altura relativa de 700 m. Os mapas de seppômen mostram escarpa marginal íngreme de 28º de declividade na borda nordeste, platô virtual com 450 m de altitude na parte central e saliência de topo com altura relativa de 250 m. Os mapas de sekkokumen apresentam forma tridimensional convexa do fundo das drenagens da área noroeste. Os mapas de kifukuryo demonstram zona de alta declividade ao longo da borda da intrusão. O índice de macro concavidade (MCI) do maciço inteiro é -0.9, indicando forma tridimensional convexa do maciço. A área nordeste do maciço tem baixo MCI de -1.1 e a área sudeste possui MCI mais alto de -0.8. A morfologia côncava da área sudeste é devido às rochas piroclásticas subvulcânicas e o nefelina sienito sob alteração do metassomatismo e hidrotermalismo. As drenagens forma um sistema radial e são íngremes e curtos com comprimento médio de 1.2 km. Na área noroeste do maciço, as drenagens têm alta declividade de 19.5° me média. Na área sudeste, as drenagens possuem baixa declividade de 10.1°. O histograma de distribuição altimétrica mostra a escarpa marginal íngreme na faixa de altitude de 50 a 450 m. A forma tridimensional geral convexa do maciço Tanguá é originada de alta resistência erosiva do nefelina sienito devido à firmeza mecânica e passividade intempérica. O maciço foi formado pela erosão diferencial do corpo intrusivo relativa ao gnaisse encaixante.
Palavras-chave: seppômen, sekkokumen, kifukuryo, GDEM, Tanguá, perfil longitudinal.

ABSTRACT - This article presents morphologic characteristics and erosive resistance of the felsic alkaline intrusive massif of Tanguá, State of Rio de Janeiro, Brazil, based on the ASTER GDEM satellite-derived topographic data. The intrusive massif has an extension of 5.5 x 7.5 km and relative height of 700 m. The summit level maps show high-angle marginal scarp with a declivity of 28° on the north-western border, virtual plateau of 450 m of altitude in the central part, and top swell with relative height of 250 m. The base level maps present convex three-dimensional form of the drainage bottom of the north-western area. The relief amount maps demonstrate high declivity zone along the intrusion border. The whole massif macro concavity index (MCI) is -0.9, indicating convex three-dimensional form of the massif. The north-western area has low MCI of -1.2 and the south-eastern area has higher MCI of -0.8. The concave morphology of the south-eastern area is due to the subvolcanic pyroclastic rocks and the nepheline syenite under the alteration of metasomatism and hydrothermalism. The drainages form a radial system and are steep and short with average length of 1.2 km. On the north-western area of the massif, the drainages have high declivity of 19.5° in average. On the south-east area, the drainages have low declivity of 10.1°. The altitude distribution histogram shows the steep marginal scarp in the altitude range of 50 to 450 m. The convex three-dimensional general form of Tanguá massif is originated from high erosive resistance of nepheline syenite because of mechanical firmness and weathering passivity. The massif has been formed by differential erosion of the intrusive body relative to the country gneiss.
Keyword: summit level, base level, relief amount, GDEM, Tanguá, longitudinal profile.

INTRODUCTION

The Tanguá felsic alkaline intrusive massif is situated at 22° 41.3'S and 42° 44.2'W, in the municipal district of Tanguá, State of Rio de Janeiro, Brazil. It is located at about 55 km to east-northeast of the city of Rio de Janeiro (Figure 1) and 12 km to east-southeast of

Petrochemical Complex of Rio de Janeiro (COMPERJ).

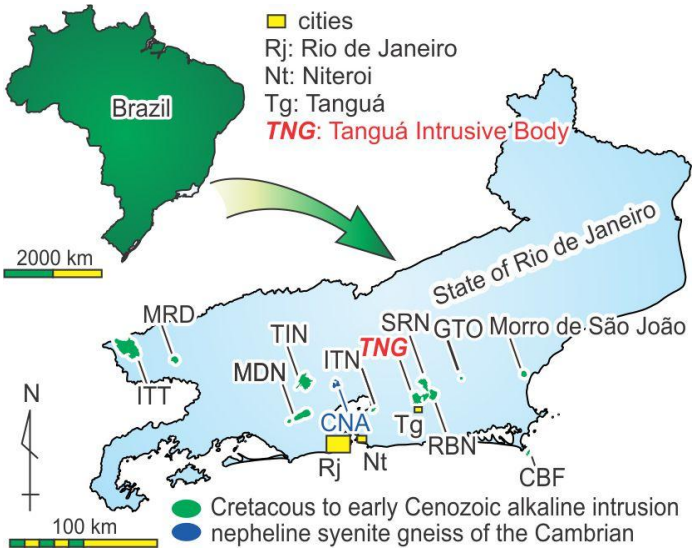

Figure 1. Locality map for the felsic alkaline intrusive massif of Tanguá, State of Rio de Janeiro, Brazil, modified from Motoki et al. (2011). ITT - Itatiaia; MRD - Morro Redondo; TNG - Tinguá; ITN - Itaúna; TNG - Tanguá; SRN - Soarinho; RBN - Rio Bonito; GTO - Morro dos Gatos; MSJ - Morro de São João; CBF - Cabo Frio Island.

At 75 km to east-northeast of the Tanguá massif, there is another similar conical alkaline intrusive rock body with a diameter of 4.5 km, called Morro de São João massif. The both are constituted mainly by nepheline syenite with local occurrences of pseudoleucite crystals (Figure 2). These rocks are strongly silica-undersaturated and highly potassic (Brotzu et al., 2007; Mota et al., 2009; Motoki et al., 2010; Sichel et al., 2012).

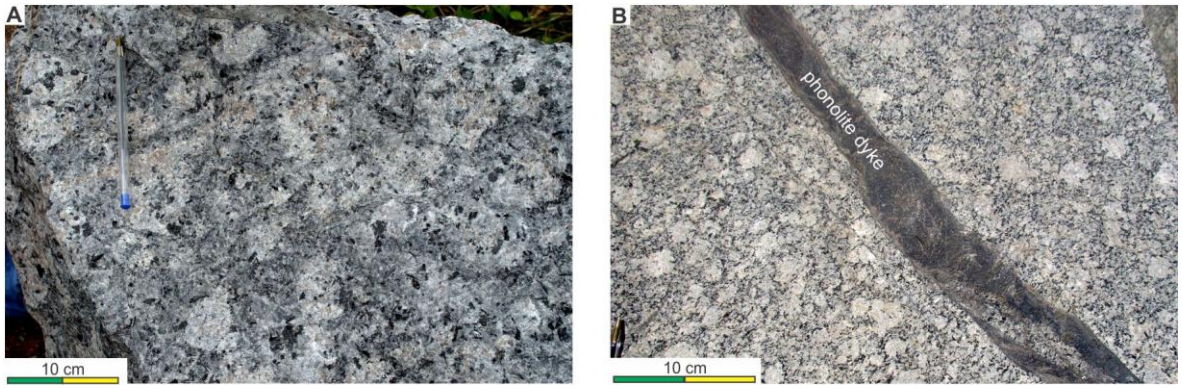

Figure 2. Pseudoleucite nepheline syenite of the felsic alkaline intrusive bodies of the State of Rio de Janeiro: A) Large pseudoleucite crystals of the Tanguá body (Motoki et al., 2010); B) Smaller pseudoleucite of the Morro de São João body (Motoki et al., 2014).

Because of the conical form, local non-scientific sources, such as the homepages of sightseeing agencies, informed as if Morro de São João massif were a volcano. However, recent studies demonstrated that the massif is constituted by coarse-grained plutonic rocks (Brotzu et al., 2007; Mota et al., 2009) and its three-dimensional morphology is widely different from volcanic edifices (Motoki et al., 2014). Therefore, Morro de São João massif is not a volcano, a massif of differential erosion of the intrusive body. The Tanguá massif has similar morphologic characteristics but no volcano urban legend has been heard.

The authors have performed morphologic analyses of Tanguá intrusive massif using summit level and base level techniques based on the ASTER GDEM satellite-derived topographic data. The present article shows the results and considers the landform origin of Tanguá massif using macro concavity index (MCI), stream-gradient index (SGI, Hack index), and area-normalised stream concavity index (SCI).

RESEARCH METHODS

The authors have adopted the following methods for the morphological analyses: 1) Summit level map; 2) Base level map; 3) Relief amount map; 4) Macro concavity index (MCI); 5) Longitudinal profile of drainages; 6) Altitude distribution histogram.

Summit level map (*seppômen*) is the virtual topographic map which reproduces the morphology before vertical erosion by drainages. This map is made up only of the highest points extracted from the original topographic map, such as peaks and crests (Motoki et al., 2008a). Base level map (*sekkokumen*) is the virtual topographic map that predicts the future morphology to be formed by lateral erosion of the present drainages. It is constructed only by the lowest points, as valley bottoms. Relief amount map (*kifukuryo*) is made up of the difference between the summit level and base level surfaces.

These virtual maps are constructed from the satellite-derived digital elevation model of ASTER GDEM (Global Digital Elevation Map) released by ERSDAC (Earth Remote Sensing Analyses Center), Japan. They are processed by the original software BAZ 1.0, Build 71, which elaborates simultaneously summit level, base level, and relief amount maps based on grid intervals of 1920 m, 960 m, 480 m, 240 m, 120 m, and 60 m. The macro concavity index (MCI) measures general form of the target massive if it is convex or concave. The details of this parameter are found in Motoki et al. (2008a; 2014) and Aires et al. (2012).

This article adopts Macro Concavity Index, called briefly MCI, in order to represent the concavity of general three-dimensional landform of massif (Motoki et al., 2012a; 2015a; b; Motoki K.F. et al., 2014). The massifs with high MCI, such as stratovolcanoes, have concave general three-dimensional form and those with low MIC, convex form. This parameter is obtained from the diagram of summit level vs. relief amount, called MCI diagram. The MCI parameter corresponds to 1000 times of the "**a**" constant of the quadric equation (y=**a**x^2+bx+c) of the second order polynomial regression.

TANGUÁ FELSIC ALKALINE INTRUSIVE BODY

The Tanguá felsic alkaline rock body is intrusive into the metamorphic basement, which is constituted by paragneiss of the Costeiro unit (Valladares et al., 2008) and orthogneiss of the Oriental Terrane (Heilbron et al., 2000; Heilbron & Machado, 2003). They were formed during late stage of the Pan-African continental collision event. The metamorphic ages range from 530 Ma to 560 Ma (Motoki, unpublished data). The gneisses are cut by silicified tectonic breccia of the latest phase of the orogeny (Motoki et al., 2011; 2012b). They are intruded by early Cretaceous mafic dykes of the continental flood basalt of Paraná Province (Stewart et al., 1996; Guedes et al., 2005; Motoki et al., 2009).

All of them are intruded by late Cretaceous to Early Cenozoic felsic alkaline bodies, such as Itatiaia (Brotzu et al., 1997), Morro Redondo (Brotzu et al., 1989), Tinguá (Derby, 1897), Mendanha (Motoki et al., 2007a), Itaúna (Motoki et al., 2008b), Tanguá, Rio Bonito, Soarinho (Motoki et al., 2010), Morro dos Gatos (Motoki et al., 2012c; Geraldes et al., 2013), Morro de São João (Brotzu et al., 2007; Mota et al., 2009), and Cabo Frio Island (Motoki & Sichel, 2008; Motoki et al., 2008c; 2013).

Some of the alkaline intrusions, as Itatiaia, Mendanha, Itaúna, Tanguá, Morro dos Gatos, and Cabo Frio Island (Motoki et al., 2007b; Sichel et al., 2008; Motoki & Sichel, 2008) have subvolcanic pyroclastic conduits filled mainly by welded tuff breccia (Motoki et al., 2008d). They are not constituents of extrusive bodies of eruptive deposits but subvolcanic intrusive rock bodies emplaced in a depth of 3 to 4 km, such as conduits, fissures, and pyroclastic dykes (Motoki & Sichel, 2006; Motoki et al., 2007c). The underground structures of that time, as magma chambers and subvolcanic conduits, are now exposed on the

Earth's surface because of regional uplift and the consequent denudation during the Early Cenozoic (Riccomini et al., 2004; Aires et al., 2012).

The Tanguá felsic alkaline intrusive body constitutes a semi-circular massif of an extension of 5.5 km x 7.5 km and relative height of 700 m. According to the pixel counting method (Motoki et al., 2007d; Geraldes et al., 2013), with the help of the original software Wilbur ver. 1.0 (Motoki et al., 2006), the distribution area of the alkaline rocks is 30 km^2.

The intrusive body is made up mainly of nepheline syenite and partially of tabular bodies of phonolite. At the western border, large pseudoleucite crystals of 5 to 10 cm in diameter are found (Figure 2A). There are two generation of phonolite, before and after the nepheline syenite intrusion (Motoki et al., 2010). The intrusive body has a flattened coffee filter-like three-dimensional form (Motoki et al., 2008d). The present exposure of Tanguá intrusion corresponds to a horizontal section of middle level of the pluton.

SUMMIT LEVEL MAPS

The Figure 3 shows summit level maps for Tanguá massif based on grid intervals of 960 m, 480 m, and 240 m. The summit level map of 960 m of grid presents smooth slope without notable characteristics. Only the largest drainage D1 is observable. This observation indicates that most of the drainages are narrower than 480 m.

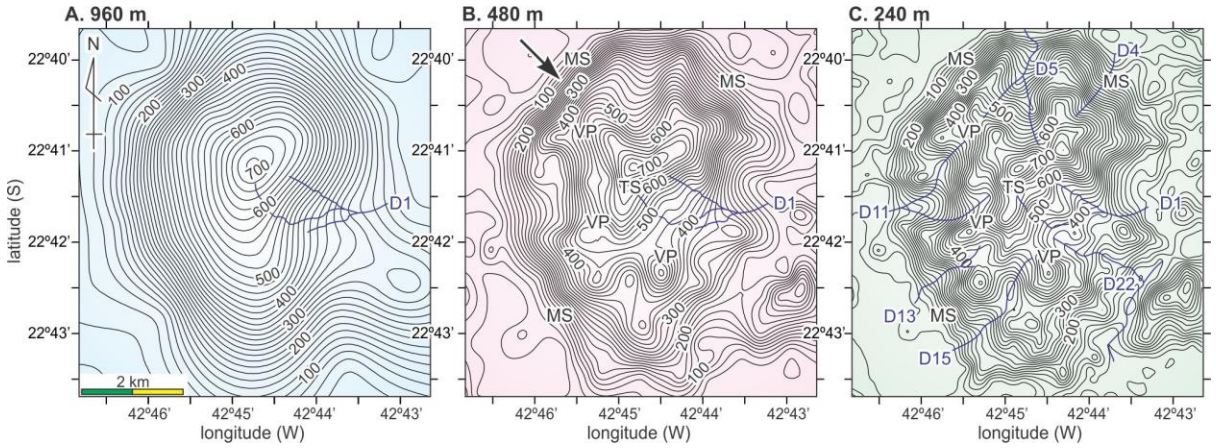

Figure 3. Summit level maps for Tanguá intrusive massif, State of Rio de Janeiro, based on grid interval of: A) 960 m; B) 480 m; C) 240 m. MS - marginal scarp; VP - virtual plateau; TS - top swell.

The summit map of 480 m of grid (Figure 3B) shows steep marginal scarp (MS), virtual plateau of about 450 m of altitude (VP), and top swell with a relative height of 250 m (TS). The virtual plateau is constituted by high crests and deep valleys. It is of erosive origin and not a remnant elevated peneplane. The marginal scarp is steep, up to 28º of declivity at the north-western slope (Figure 3B, arrow). These morphological units are observed characteristically in the felsic alkaline massifs of this region (Silva, 2010). However, the marginal scarp of the southeast slope of Tanguá massif is no so steep.

The map of 240 m (Figure 3C) shows four parallel drainages wider than 120 m with strike of N40°E, D5, D11, D13, and D15. This direction is parallel to one of the fracture systems of the metamorphic basement. The outlets of the drainages D5, D11, and D13 have small hills with a relative height of 50m and horizontal extension of 100 to 300 m, suggesting large block landslide.

The Figure 4A shows horizontal silhouette of the field photo taken from north-western direction of the massif. It is similar to the summit level profile, with well expressed the marginal scarp (MS) and virtual plateau (VP) on the symmetric profile. The top swell is not observed in this photograph because of the angle. On the other hand, the summit level cross section of the perpendicular direction shows an asymmetric profile showing low-angle south-eastern slope (Figure 4B).

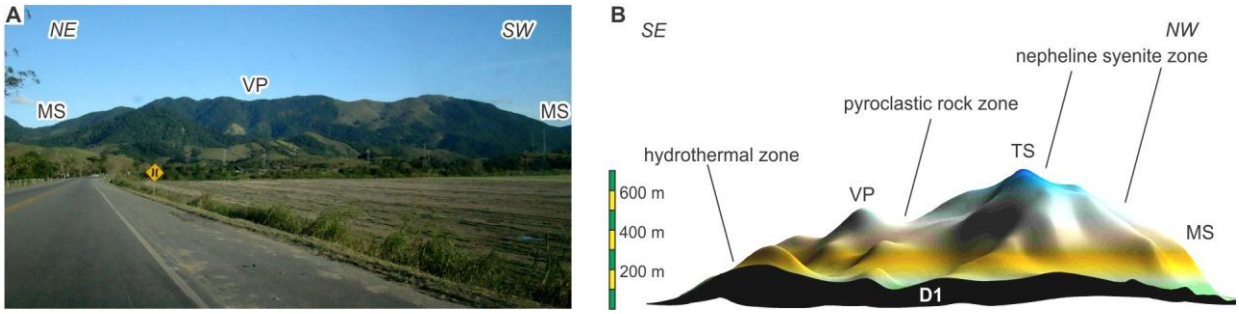

Figure 4. The marginal scarp (MS), the virtual plateau (VP), and the top swell (TS) expressed on the silhouette of Tanguá felsic alkaline intrusive massif: A) Field photograph showing NE-SW section; B) Summit level surface of the 240 m grid interval demonstrating NW-SE section.

The south-eastern slope is constituted exceptionally by subvolcanic pyroclastic rocks and the nepheline syenite under strong effects of metassomatic and hydrothermal alteration. The hydrothermalism is observed typically in the fluorite veins. This mineral is in extraction by the EMITANG (Mining Company of Tanguá).

BASE LEVEL MAPS AND RELIEF AMOUNT MAPS

The Figure 5 presents base level maps of the grid of 960 m, 480 m, and 240 m. The map of 960 m shows conical virtual form without drainages (Figure 5A). The map of 480 m of grid (Figure 5B) show virtual plateau, top swell and marginal scarp. In comparison with the summit level maps they are not so clear. The erosion effect of D1 is observed.

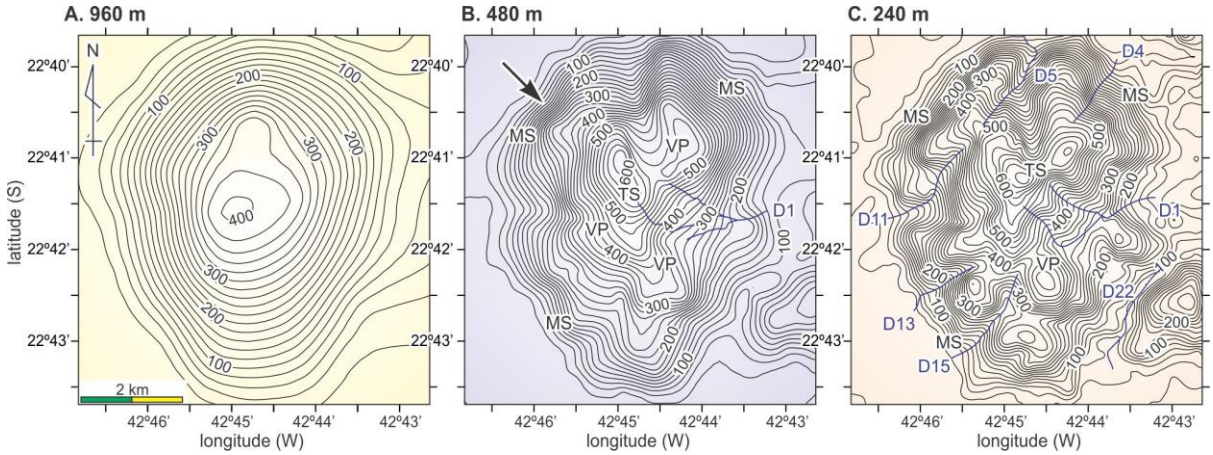

Figure 5. Base level maps for Tanguá massif, State of Rio de Janeiro, Brazil, based on grid interval of: A) 960 m; B) 480 m; C) 240 m. MS - marginal scarp; VP - virtual plateau; TS - top swell.

The map of 240 m mesh interval (Figure 5C) shows more expressively the virtual plateau, top swell, and marginal scarp. The marginal scarp of the north-western border is steep, with a declivity of 28° (Figure 5B, arrow). These observations indicate that the nepheline syenite is highly resistant to vertical erosion of drainages. The drainage D4, D5, D11, D13, D15, and D22 form a parallel system with the orientation to N40°E. They are wider than 120 m and appear more clearly than the summit level map.

The Figure 6 presents relief amount maps of the grid intervals of 960 m, 480 m, and 240 m (coloured background) which are overlain by the summit level maps of the same grid interval (black contour curves). The map of 960 m of grid (Figure 6A) shows high declivity zones (blue and white zones) along the intrusion border. These characteristics are common in the felsic alkaline intrusive massifs (Silva et al., 2000). The maps of 480 m and 240 m of grid (Figure 6B, C) show no notable features.

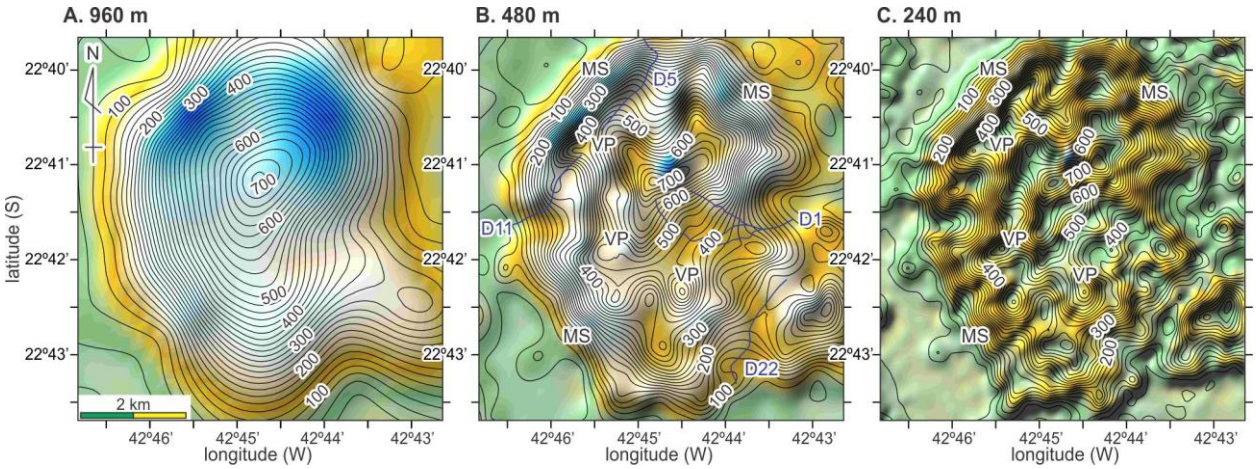

Figure 6. Relief amount maps (coloured background) superposed by the summit level surfaces (black counter curves) for Tanguá intrusive massif, State of Rio de Janeiro based on the grid of: A) 960 m; B) 480 m; C) 240 m. MS - marginal scarp; VP - virtual plateau.

MACRO CONCAVITY INDEX

Tanguá massif has remarkable morphologic contrast between the north-western and south-eastern areas (Figure 4B), so the analyses of macro concavity index, MCI, have performed for: 1) Whole massif; 2) North-western area; 3) South-eastern area (Figure 7A).

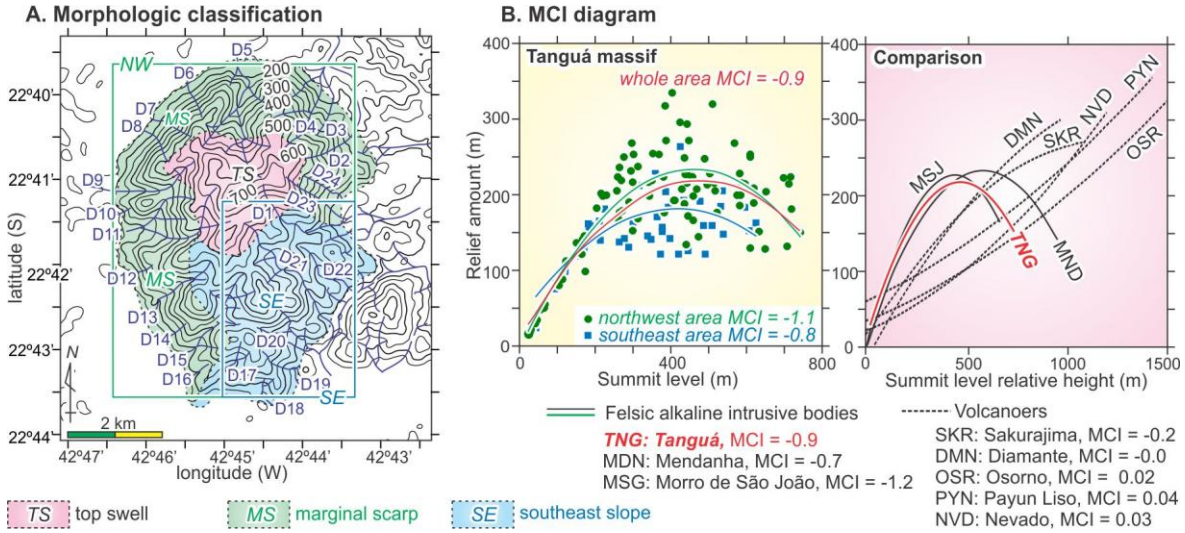

Figure 7. MCI (Macro Concavity Index) diagram based on the grid of 488 m for Tanguá massif: A) Morphologic classification map; B) MCI diagrams of the north-western area (green), south-western area (blue), and whole area (red). The data for the volcanic edifices are after Motoki et al. (2012a; 2014).

The MCI for the whole Tanguá massif is -0.9 (Figure 7B). The negative value is common in the felsic alkaline intrusive bodies of this region. The MCI for the north-western area is strongly negative, -1.1, which is comparable with -1.2 of the Morro de São João. The convex landform is attributed to strong erosive resistance of nepheline syenite (Motoki et al., 2008a; Petrakis et al., 2010).

On the other hand, the MCI for the south-eastern area is -0.8. The higher value should be due to the erosive vulnerability of the pyroclastic rocks (Figure 8A) and the nepheline syenite with metassomatic and hydrothermal alterations. The wide variation of Ba and Sr of Tanguá nepheline syenite (Motoki et al., 2010) indicates strong and heterogeneous fluid activities (Figure 8B).

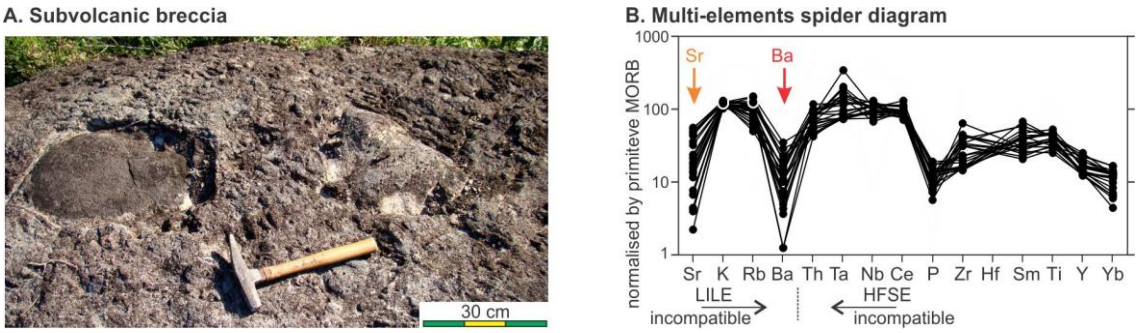

Figure 8. Erosive vulnerability of the south-eastern area: A) Pyroclastic rock with semi-rounded boulder-size trachytic clasts at drainage D1 (Figure 7A); B) Multi-element spider diagram for the nepheline syenite samples of Tanguá intrusion showing wide variation of Ba and Sr. The geochemical data are after Motoki et al. (2010).

DRAINAGE SYSTEM

In total, 24 drainages of the Tanguá intrusive massif are analysed. The drainages form a radial system, and are generally short, steep, and shallow, with poorly developed branches. The average length is 1.23 km, relative height is 301 m, and declivity is 16.3°.

The drainages D1, D15, D17, D18, D19, D20, D21, and D22 are on the south-eastern area of the massif and the other ones are on the northwest area (Figure 7A). The drainages of the north-western area are steeper, with average declivity of 19.5°, and those of the southeaster slope are gentler, 10.1°. The steepest drainage is D6 of the north-western area, with declivity of 28.7°. Most of them have almost straight longitudinal profile without relevant knickpoint (Figure 9A). The short drainages tend to be steep and the long ones are gentle. The D1 and D21 are two longest drainages and the longitudinal profile is slightly concave at their stream head. The above-mentioned features are commonly observed in the drainages of the felsic alkaline intrusive massifs of this region (Silva, 2010; Motoki et al., 2008a; 2014). The D5 and D9 are on the north-western area, nevertheless they have gentle gradient. This observation is attributed to the fact that they are developed along one of the regional Cenozoic parallel fracture system (Aires et al., 2012).

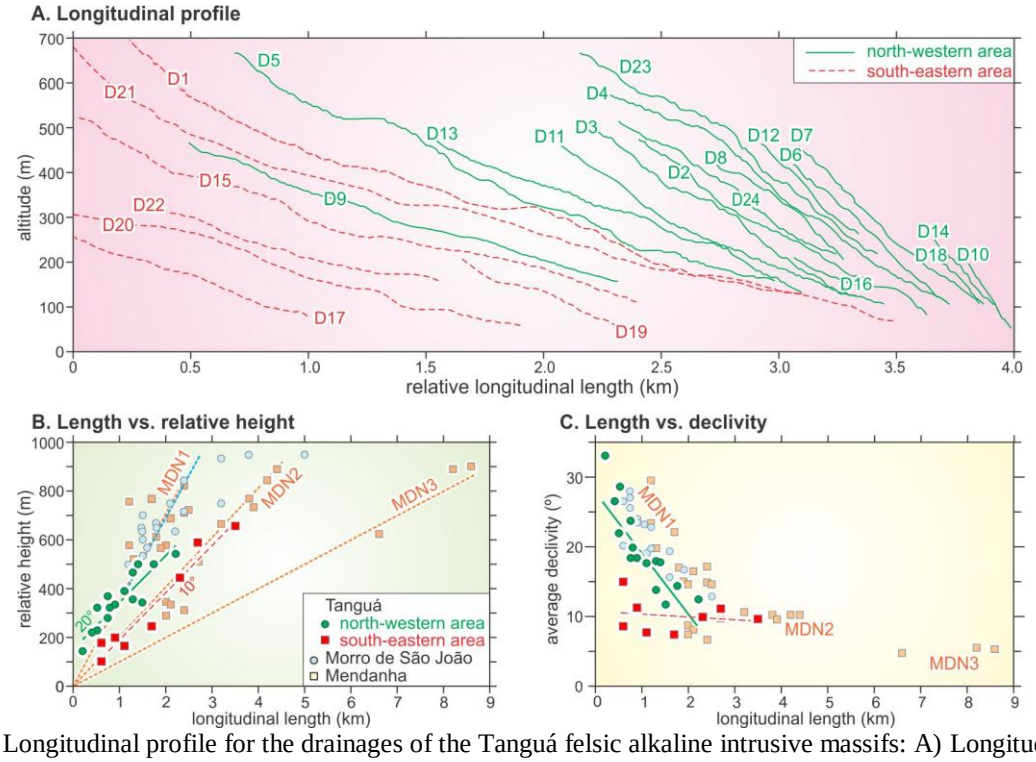

Figure 9. Longitudinal profile for the drainages of the Tanguá felsic alkaline intrusive massifs: A) Longitudinal cross section; B) Stream length vs. relative height; C) Stream length vs. average declivity. The data of the Mendanha and Morro de São João massifs are after Motoki et al. (2008a; 2014).

For the analyses of the erosive resistance of the base rock, the authors have adopted stream-gradient index (SGI), called also Hark index, and stream concavity index (SCI). The stream-gradient index represents degree of declivity of determined span (Hack, 1973).

$$SGI = (\Delta H/\Delta L) \times L$$

SGI: stream-gradient index (Hack index).
ΔH: altitude difference in the span.
ΔL: longitudinal distance of the span.
L: upstream distance

This parameter is stable within a span of simple erosion. Drastic changes of this parameter are attributed to the change of erosive conditions, such as vertical movement of active fault and different base rocks. SGI is useful for neotectonic studies (e.g. Seeber & Gornitz, 1983; Kirby et al., 2003; Etchebehere et al., 2004; Sougnez & Vanacker, 2011).

Most of the drainages of the north-western area show linear increase of SGI from upstream to downstream (Figure 10A). That is, their downstream is steeper than the model of Hack (1973). The longitudinal profiles are rather straight than concave, which is common in the felsic alkaline intrusive massifs.

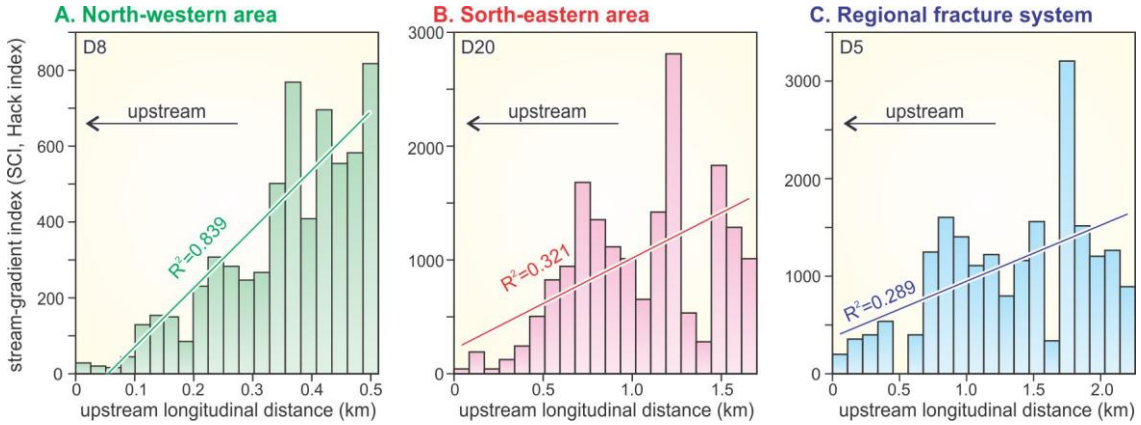

Figure 10. Longitudinal variation of the stream-gradient index (SGI, Hack index) for the drainages of the Tanguá massif: A) D8 of the north-western area; B) D20 of the south-eastern area; C) D5 developing along the NE-SW fracture system. The stream-gradient index values are natural and not area-normalized.

The drainages of the south-eastern area also show similar tendency but less relevant, and the SGI increase pattern is not so linear (Figure 10B). The drainages D5 and D9 are present on the north-western area. They are developed along the NW-SE regional parallel fracture system. Because of the base rock physical debility, the SGI increasing pattern is not as clear as the other drainages of the north-eastern area (Figure 10C).

The area-normalized stream concavity index (SCI; Demoulin, 1998; Zaprowski et al., 2005) represents longitudinal profile concavity of target drainage. This parameter is useful for neotectonic studies (Wells et al., 1988; Kirby & Whipple, 2001; Rãdoane, et al., 2003).

The drainages of Tanguá massif have low SCI and about 40% of them have negative value, showing convex general form. The drainages of the north-western area have average SCI of 0.025. It is significantly lower than those of the south-eastern area, in average 0.077. The straight to convex stream profiles are attributed to high erosive resistance of unaltered nepheline syenite.

These drainages have a good correlation between the SCI and linear increasing pattern of the stream gradient-index on the longitudinal variation diagram. The latter parameter is represented by the R^2 of the Figure 10. On the diagrams of area-normalised SGI and SCI, the drainages with high R^2 tend to have convex profile with low SCI, such as the D8 and D16 (Figure 11A). The drainage D5 has exceptionally low SCI because of the regional fracture system. The long drainages have concave profiles with high SCI (Figure 11B).

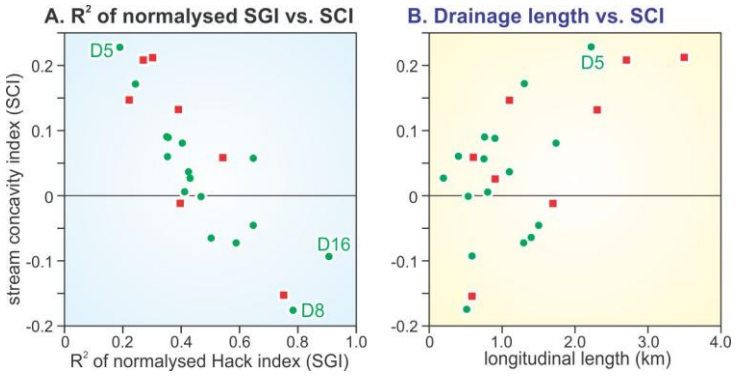

Figure 11. Variations of the area-normalised stream concavity index (SCI) for the drainages of Tanguá intrusive massif according to: A) R^2 of the area-normalized (length=1.0; relative height=1.0) SGI diagram (Figure 10); B) Longitudinal length.

ALTITUDE DISTRIBUTION HISTOGRAM

The altitude distribution histogram for Tanguá massif shows church bell-like patterns (Figure 12A, B) because of the steep marginal scarp in the altitude ranging from 50 to 450 m, the virtual plateau with altitude of 450 to 500 m, and the top swell with relative height of 250 to 300 m. The marginal scarp of south-eastern area is situated in lower altitude ranging from 50 to 350 m. This pattern is commonly observed in the felsic alkaline intrusive massifs of this region (Figure 12C, D). These observations corroborate the arguments based on the summit level (Figure 3), base level (Figure 5), and relief amount maps (Figure 6).

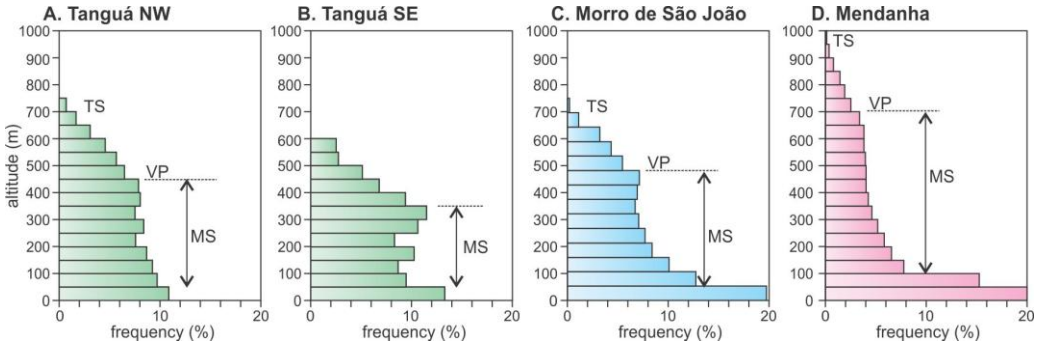

Figure 12. Altitude distribution histogram for the felsic alkaline intrusive massifs of the State of Rio de Janeiro. A) North-western area of Tanguá; B) South-eastern area of Tanguá; C) Morro de São João; D) Mendanha. The data of the Morro de São João and the Mendanha are after (Motoki et al., 2008a; 2014). MS - marginal scarp; VP - virtual plateau; TP - top swell.

LANDFORM ORIGIN

Tanguá massif has morphologic characteristics similar to those of the Morro de São João, with minor differences. The virtual plateau is not so sharp because of low declivity of the south-eastern area. There are deep drainages which follow the NE-SW regional parallel fracture system (Figure 13, arrows).

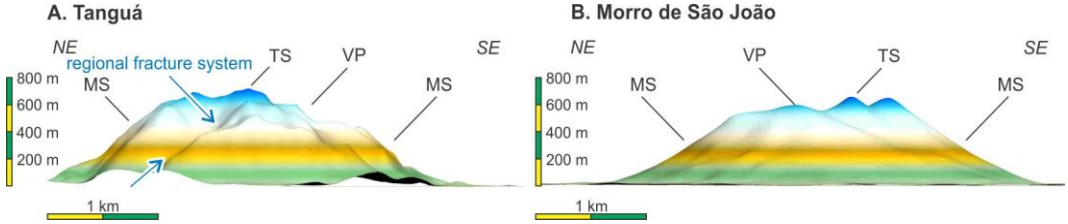

Figure 13. Comparative cross section of the summit level surface based on the grid interval of 240 m for the felsic alkaline intrusive massifs: A) Tanguá massif from the north-west (present data); B) Morro de São João massif form the north-west (Motoki et al., 2014). MS - marginal scarp; VP - virtual plateau; TS - top swell.

Although the silhouette of Tanguá massif is similar to young stratovolcanoes, its three-dimensional form is widely different: 1) High-declivity slope on the mountain foot; 2) Absence of volcanic crater; 3) Convex general form with negative MCI of -0.9.

The convex general form of the massif is attributed to high erosive resistance of nepheline syenite. The failure stress by uniaxial compression of the syenitic rocks of this region is about 170 MPa (Petrakis et al., 2010), being much higher than of granitic rocks, approximately 120 MPa. Although the nepheline syenite is vulnerable to chemical weathering under the humid tropical climate condition, the clay-rich impermeable regolith protects form surface water percolation into the rock body, the effect called weathering passivity (Motoki et al., 2008a). It is considered that Tanguá massif is originated from differential erosion due to the erosive resistance of the nepheline syenite (Figure 14). The stratovolcano-like circular morphology corresponds to an art of the nature.

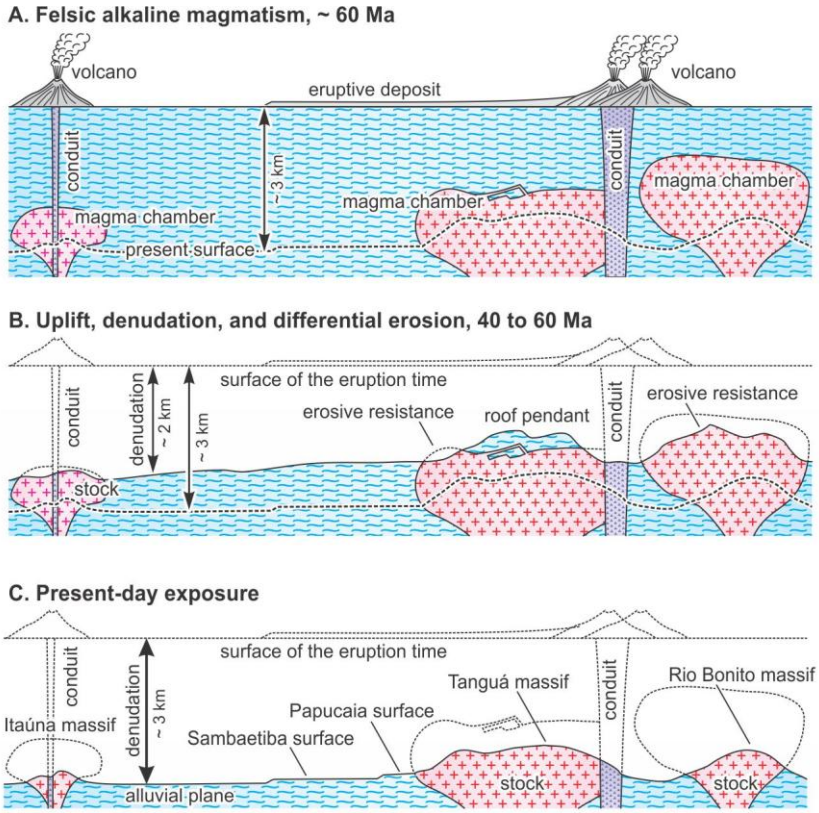

Figure 14. Schematic geologic section showing regional denudation and alkaline massif formation processes of Tanguá area: A) Volcanic eruptions and magma intrusions at Early Cenozoic, ca. 60 Ma; B) Tectonic uplift, regional denudation, and differential erosion in a period of 60 to 40 Ma; C) Present-day exposure with alkaline intrusive massifs and subvolcanic pyroclastic conduits.

CONCLUSION

The morphologic analyses of Tanguá felsic alkaline intrusive massif, with the help of summit level and base level techniques based on the ASTER GDEM has lead the authors to the following conclusions.

1. Tanguá intrusive massif has an extension of 5.5 x 7.5 km and relative height of 700 m, with distribution area of 30 km^2.
2. The summit level maps show steep marginal scarp with a declivity of 28º, virtual plateau of 450 m of altitude, and top swell with a relative height of 250 m.
3. The base level maps present convex three-dimensional form of the north-western area. The relief amount maps demonstrate high declivity zone along the intrusion border.

4. The MCI for the whole massif is -0.9, indicating convex three-dimensional general form. The north-western area has low MCI of -1.2, being convex. The south-eastern area has higher MCI of -0.8, being concave. The concave form is due to the pyroclastic rocks and the nepheline syenite altered by metasomatism and hydrothermalism.
5. The drainages are short and steep, in average 1.2 km long, forming a radial system. Those of the north-western area are almost straight in longitudinal profile with average declivity of 19.5°. Those of the south-eastern area are slightly concave on their stream head, with average declivity of 10.1°.
7. The altitude distribution histogram shows steep marginal scarp in altitude range of 50 to 450 m, the virtual plateau with altitude of 450 to 500 m, and the top swell with relative height of 250 to 300 m.
8. The convex three-dimensional form of Tanguá massif is originated from high erosive resistance of the nepheline syenite due to mechanical firmness and weathering passivity. This massif has been formed by differential erosion of the nepheline syenite intrusion relative to country metamorphic basement.

ACKNOWLEDGEMENT

The contents of this article correspond to an advanced research started from the Master Degree thesis of Samuel da Silva, one of the authors, at the Federal Fluminense University, Niterói, State of Rio de Janeiro, Brazil. The authors are grateful to FAPERJ (scientific financial support foundation of the State of Rio de Janeiro) and PETROBRAS (Brazilian national petroleum company) for the financial supports.

REFERENCE

1. AIRES, J.R.; MOTOKI, A.; MOTOKI, K.F.; MOTOKI, D.F.; RODRIGUES, J.G. Geomorphological analyses of the Teresópolis Plateau and Serra do Mar Cliff, State of Rio de Janeiro, Brazil with the help of summit level technique and ASTER GDEM, and its relation to the Cenozoic tectonism. **Anuário do Instituto de Geociências da Universidade Federal do Rio de Janeiro**, v. 35, n. 2, p. 105-123, 2012.

2. BROTZU, P.; BECCALUVA, L.; CONTE, A.; FONSECA, M.; GARBARINO, C.; GOMES, C.B., LEONG, R.; MACCIOTTA, G.; MANSUR, R.L.; MELLUSO, L.; MORBIDELLI, L.; RUBERTI, E.; SIGOLO, J.B.; TRAVERSA, G.; VALENÇA, J.G. Petrological and geochemical studies of alkaline rocks from continental Brazil. The syenitic intrusion of Morro Redondo, RJ. **Geochimica Brasiliensis**, v. 3, p. 63-80, 1989.

3. BROTZU, P.; GOMES, C. B.; MELLUSO, L.; MORBIDELLI, L.; MORRA, V.; RUBERTI, E. Petrogenesis of coexisting SiO_2-undersaturated to SiO_2-oversaturated felsic igneous rocks: the alkaline complex of Itatiaia, southern eastern Brazil. **Lithos**, v. 40, p. 133-156, 1997.

4. BROTZU, P.; MELLUSO, L.; BENNIO, L.; GOMES, C.B.; LUSTRINO, M.; MORBIDELLI, L.; MORRA, V.; RUBERTI, E.; TASSINARI, C.; D'ANTONIO, M. Petrogenesis of the Early Cenozoic potassic alkaline complex of Morro de São João, southeastern Brazil. **Journal of South American Earth Sciences**, v. 24, p. 93-115, 2007.

5. DEMOULIN, A. Testing the tectonic significance of some parameters of longitudinal river profiles: the case of the Ardenne (Belgium, NW Europe), **Geomorphology**, n. 24, p. 189-208, 1998.

6. DERBY, O.A. On nepheline-rocks in Brazil - part II. The Tinguá Mass. **The Quarterly Journal of the Geological Society *of* London**, v. 47, p. 251-265, 1897.

7. ETCHEBEHERE, M.L.; FULFARO, V.J.; PERINOTTO, J.A.J. Aplicação do Índice .Relação Declividade-Extensão - RDE. na Bacia do Rio do Peixe (SP) para Detecção de Deformações Neotectônicas. **Revista do Instituto de Geociências - USP**, Série Científica, v. 4, n.2, p. 43-56, 2004.

8. GERALDES, M.C.; MOTOKI, A.; VARGAS, T.; IWANUCH, W.; BALMANT, A.; MOTOKI, K.F. Geology, petrography, and emplacement mode of the Morro dos Gatos alkaline intrusive rock body, State of Rio de Janeiro, Brazil. **Geociências**, Rio Claro, v. 32, n. 4, p. 625-639, 2013.

9. GUEDES, E.; HELIBRON, M.; VASCONCELOS, P.M.; VALERIANO, C.M.; ALMEIDA, J.C.H.; TEIXEIRA, W.; THOMÁZ FILHO, A. K-Ar and $^{40}Ar/^{39}Ar$ ages of dykes emplaced in the on-shore basement of the Santos Basin, Resende area, SE. Brazil: implications for the south Atlantic opening and Tertiary reactivation. **Journal of South American Earth Sciences**, v. 18, p. 371-182, 2005.

10. HACK, J. T. Stream-profile analysis and stream-gradient index. **Journal of Research of the United States Geological Survey**, v. 1, n. 4, p. 421-429, 1973.

11. HEILBRON, M. & MACHADO, N. Timing of terrane accretion in the Neoproterozoic-Eopaleozoic Ribeira orogen (se Brazil). **Precambrian Research,** v. 125, p. 87-112, 2003.

12. HEILBRON, M.; MOHRIAK, W.; VALERIANO, C.M.; MILANI, E.; ALMEIDA, J.C.A., TUPINAMBÁ, M. From collision to extension: the roots of the southeastern continental margin of Brazil. In: Mohriak, W.U. and Talwani, M. (Eds.), **Geophysical Monograph**, American Geophysical Union, v. 115, p. 1-32, 2000.

13. KIRBY, E.; WHIPPLE, K. Quantifying differential rock-uplift rates via stream profile anaylsis. **Geology**, v. 29-5, p. 415–418, 2001.

14. KIRBY, E.; WHIPPLE, K.X.; TANG, W.; CHEN, Z. Distribution of active rock uplift along the eastern margin of the Tibetan Plateau: Inferences from bedrock channel longitudinal profile. **Journal of Geophysical Research**, Solid Earth, electronic edition, v. 108, n. B4, DOI: 10.1029/2001JB00086, 2003.
15. MOTA, C.E.M.; GERALDES, M.C.; ALMEIDA, J.C.H.; VARGAS, T.; SOUZA, D.M.; LOUREIRO, R.O.; SILVA, A.P. Características Isotópicas (Nd e Sr), Geoquímicas e Petrográficas da Intrusão Alcalina do Morro de São João: Implicações Geodinâmicas e Sobre a Composição do Manto Sublitosférico. **Revista do Instituto de Geociências - USP, Série Científica.**, São Paulo, v. 9, n. 1, p. 85-100, 2009.
16. MOTOKI, A. & SICHEL, S.E. Avaliação de aspectos texturais e estruturais de corpos vulcânicos e subvulcânicos e sua relação com o ambiente de cristalização, com base em exemplos do Brasil, Argentina e Chile. **REM-Revista Escola de Minas**, Ouro Preto, v. 59, n. 1, p. 13-23, 2006.
17. MOTOKI, A. & SICHEL, S.E. Hydraulic fracturing as a possible mechanism of dyke-sill transitions and horizontal discordant intrusions in trachytic tabular bodies of Arraial do Cabo, State of Rio de Janeiro, Brazil. **Geofísica Internacional**, Mexico City, v. 47, v. 1, p. 13-25, 2008.
18. MOTOKI, A.; ZUCCO, L.L.; SICHEL, S.E.; AIRES, J.R.; PETRAKIS, G.H. Desenvolvimento da técnica para especificação digital de cores e a nova nomenclatura para classificação de rochas ornamentais com base nas cores medidas. **Geociências**, Rio Claro, v. 25, n. 4, p. 403-415, 2006.
19. MOTOKI, A.; SOARES, R.; NETTO, A.M.; SICHEL, S.E.; AIRES, J.R.; LOBATO, M. Geologic occurrence shape of pyroclastic rock dykes in the Dona Eugênia River Valley, Municipal Park of Nova Iguaçu, Rio de Janeiro. **Geociências**, Rio Claro, v. 26, n. 1, p. 67-82. 2007. (a)
20. MOTOKI, A.; SOARES, R.; LOBATO, M.; SICHEL, S.E.; AIRES, J.R. Weathering fabrics in felsic alkaline rocks of Nova Iguaçu, State of Rio de Janeiro, Brazil. **REM-Revista Escola de Minas**, Ouro Preto, v. 60, n. 3, p. 451-458, 2007. (b)
21. MOTOKI, A.; SOARES, R.; NETTO, A.M.; SICHEL, S.E.; AIRES, J.R.; LOBATO, M. Genetic reconsideration of the Nova Iguaçu Volcano model, State of Rio de Janeiro, Brazil: eruptive origin or subvolcanic intrusion? **REM-Revista Escola de Minas**, Ouro Preto, v. 60, n. 4, p. 583-592. 2007. (c)
22. MOTOKI, A.; PETRAKIS, G.H.; SOARES, R.S.; SICHEL, S.E.; AIRES, J.R. New method of semi-automatic modal analyses for phenocrysts of porphyritic rocks based on quantitative digital colour specification technique. **Revista Escola de Minas**, Ouro Preto, v. 60, n. 1, p. 13-20. 2007. (d)
23. MOTOKI, A.; PETRAKIS, G.H.; SICHEL, S.E.; CARDOSO, C.E.; MELO, R.C.; SOARES, R.S.; MOTOKI, K.F. Landform origin of the Mendanha Massif, State of Rio de Janeiro, Brazil, based on the geomorphological analyses by summit level map technique. **Geociências**, Rio Claro, v. 27, n. 1, p. 99-115, 2008. (a)
24. MOTOKI, A., SICHEL, S.E., SOARES, R.S., NEVES, J.L.P., AIRES, J.R. Geological, lithological, and petrographical characteristics of the Itaúna Alkaline Intrusive Complex, São Gonçalo, State of Rio de Janeiro, Brazil, with special attention of its emplace mode. **Geociências**, Rio Claro, v. 27, n. 1, p. 33-44, 2008. (b)
25. MOTOKI, A.; SICHEL, S.E.; SAVI, D.C.; AIRES, J.R. Corpos tabulares de intrusão subhorizontal discordante em torno do sienito da Ilha de Cabo Frio, RJ, e seu mecanismo de posicionamento. **Geociências**, Rio Claro, v. 27, n. 2, p. 207-218, 2008. (c)
26. MOTOKI, A.; SICHEL, S.E.; SOARES, R.S.; AIRES, J.R.; SAVI, D.C.; PETRAKIS, G.H.; MOTOKI, K.F. Vent-filling pyroclastic rocks of the Mendanha, the Itaúna, and the Cabo Frio Island, State of Rio de Janeiro, Brazil, and their formation process based of the conduit implosion model. **Geociências**, Rio Claro. v. 27, n. 3, p. 451-467, 2008. (d)
27. MOTOKI, A.; SICHEL, S.E.; PETRAKIS, G.H. Genesis of the tabular xenoliths along contact plane of the mafic dykes of cabo frio area, state of Rio de Janeiro, Brazil: Thermal delamination or hydraulic shear fracturing? **Geociências**, Rio Claro, v. 28, n. 1, p. 15-26, 2009.
28. MOTOKI, A.; SICHEL , S.E.; VARGAS, T.; AIRES, J.R.; IWANUCH, W.; MELLO, S.L.M.; MOTOKI, K.F.; SILVA, S.; BALMANT, A.; GONÇALVES, J. Geochemical evolution of the felsic alkaline rocks of Tanguá, Rio Bonito, and Itaúna intrusive bodies, State of Rio de Janeiro, Brazil. **Geociências**, Rio Claro, v. 29, n. 3, p. 291-310, 2010.
29. MOTOKI, A.; VARGAS, T.; IWANUCH, W.; SICHEL, S.E.; BALMANT, A.; AIRES, J.R. Tectonic breccia of the Cabo Frio area, State of Rio de Janeiro, Brazil, intruded by Early Cretaceous mafic dyke: Evidence of the Pan-African brittle tectonism ? **REM-Revista Escola de Minas**, Ouro Preto, v. 64, n. 1, p. 25-36, 2011.
30. MOTOKI, A.; CAMPOS, T.F.C.; FONSECA, V.P.; MOTOKI, K.F. Subvolcanic neck of Cabugi Peak, State of Rio Grande do Norte, Brazil, and origin of its landform. **REM-Revista Escola de Minas**. Ouro Preto, v. 65, n. 2, p. 195-206, 2012. (a)
31. MOTOKI, A.; VARGAS, T.; IWANUCH, W.; MELO, D.P.; SICHEL, S.E.; BALMANT, A.; AIRES, J.R.; MOTOKI, K.F. Fossil earthquake evidenced by the silicified tectonic breccia of the Cabo Frio area, State of Rio de Janeiro, Brazil, and its bearings on the genesis of stick-slip fault movement and the associated amagmatic hydrothermalism. **Anuário do Instituto de Geociências da Universidade Federal do Rio de Janeiro**, Rio de Janeiro, v. 35, n. 2, p. 124-139, 2012. (b)
32. MOTOKI, A.; GERALDES, M.C.; IWANUCH, W.; VARGAS, T.; MOTOKI, K.F.; BALMANT, A.; RAMOS, M.N. The pyroclastic dyke and welded crystal tuff of the Morro dos Gatos alkaline intrusive complex, State of Rio de Janeiro, Brazil. **REM-Revista Escola de Minas**, Ouro Preto, v. 65, n. 1, p. 35-45, 2012. (c)
33. MOTOKI, A.; ARAÚJO; A.L.; SICHEL, S.E.; MOTOKI, K.F.; SILVA, S. Nepheline syenite magma differentiation process by continental crustal assimilation for the Cabo Frio Island intrusive complex, State of Rio de Janeiro, Brazil. **Geociências**, Rio Claro, v. 32, n. 2, p. 195-218, 2013.
34. MOTOKI, A.; SILVA, S.; SICHEL, S.E.; MOTOKI, K.F. Geomorphological analyses by summit level and base level maps based on the ASTER GDEM for Morro de São João felsic alkaline Massif, State of Rio de Janeiro, Brazil. **Geociências**, Rio Claro, v. 33, n. 1, p. 11-25, 2014.
35. MOTOKI, A.; MOTOKI, K.F.; SICHEL, S.E.; SILVA, S.; AIRES, J.R. Principle and geomorphological applicability of summit level and base level technique using ASTER GDEM satellite-derived data and the original software Baz. **Acta Scientiarum Technology**, 2015. (a) (in press)
36. MOTOKI, A.; SICHEL, S.E.; SILVA, S.; MOTOKI, K.F.; RIBEIRO, A.K. Drainage erosion and concave landform of Tijuca gneissic massif, State of Rio de Janeiro, Brazil, with the help of summit level and base level technique based on ASTER GDEM. **Geociências**, 2015. (b) (in press).
37. MOTOKI, K.F.; MOTOKI, A.; SICHEL, S.E. Gravimetric structure for the abyssal mantle exhumation massif of Saint Peter and Saint Paul Peridotite Ridge, Equatorial Atlantic Ocean, and its relation to the active uplift driving force. **Anais de Academia Brasileira de Ciências**, v. 86, n. 2, p. 395-412, 2014.
38. PETRAKIS, G.H.; MOTOKI, A.; SICHEL, S.E.; ZUCCO, L.L.; AIRES, J.R.; MELLO S.L.M. Ore geology of special quality gravel and artificial sand: exemples of alkaline syenite of Nova Iguaçu, State of Rio de Janeiro, and rhyolite of

Nova Prata, State of Rio Grande do Sul, Brazil. **Geociências**, Rio Claro, v. 29, n. 1, p. 21-32, 2010.
39. RÃDOANE, M.; RÃDOANE, N.; DUMITRIU, M. Geomorphological evolution of longitudinal river profiles in the Carpathians. **Geomorphology**, v. 50, p. 293-306, 2003.
40. RICCOMINI, C.; SANT'ANNA, L.G.; FERRARI, A.L. Evolução geológica do rift continental do Sudeste do Brasil. In Mantesso-Neto, V., Bartorelli, A., Carneiro, C.D.R., Brito-Neves, B.B. Ed. **Geologia do Continente Sul-Americno: Evolução da obra de Fernando Flávio Marques de Almeida**. São Paulo. Editora Beca, p. 385-405, 2004.
41. SEEBER, L.; GORNITZ, V. River profiles along the Himalayan arc as indicators of active tectonics. **Tectonophysics**, v. 92, n. 1, p. 335-367, 1983.
42. SICHEL, S.E.; MOTOKI, A.; SAVI, D.C.; SOARES, R.S. 2008. Subvolcanic vent-filling welded tuff breccia of the Cabo Frio Island, State of Rio de Janeiro, Brazil. **REM-Revista Escola de Minas**, Ouro Preto, v. 61, n. 4, p. 423-432, 2008.
43. SICHEL, S.E.; MOTOKI, A.; IWANUCH, W.; VARGAS, T.; AIRES, J.R.; MELO, D.P.; MOTOKI, K.F.; BALMANT, A.; RODRIGUES, J.G. Fractionation crystallisation and continental crust assimilation by the felsic alkaline rock magmas of the State of Rio de Janeiro, Brazil. **Anuário do Instituto de Geociências da Universidade Federal do Rio de Janeiro**, Rio de Janeiro, v. 35, n. 2, p. 84-104,.2012.
44. SILVA, S. **Interpretação morfológica baseada nas tecnicas de seppômen e sekkokumen dos maciços alcalinos do Estado do Rio de Janeiro**. Niterói, 2010, 123 p. **Thesis** (Master in Geology) - Instituto de Geociências, Universiade Federal Fluminense. (unpublished)
45. SOUGNEZ, N.; VANACKER, V. The topographic signature of Quaternary tectonic uplift in the Ardennes massif (Western Europe). **Hydrology and Earth System Sciences**, v. 15, p. 1095-1107, 2011.
46. STEWART, S.; TURNER, S.; KELLEY, S.; HAWKESWORTH, C.; KRISTEIN, L.; MANTOVANI, M. 3D - $^{40}Ar/^{39}Ar$ geochronology in Paraná continental flood basalt province. **Earth Planet, Science Letters**. v. 143, p. 95-109, 1996.
47. VALLADARES, C.S.; MACHADO, N.; HEILBRON, M.; DUARTE, B.P.; GAUTHIER, G. Sedimentary provenance in the central Ribeira belt based on laser-ablation. **Gondwana Research**, v. 13, p. 516–526, 2008.
48. WELLS, S.G.; BULLAR, T.F.; MENGES, C.M.; DRAKE, P.G.; KARA, P.A.; KELSON, K.I.; RITTER, J.B.; WESLING, J.R. Regional variations in tectonic geomorphology along a segmented convergent plate boundary, Pacific coast of Costa Rica. **Geomorphology**, v. 1, p. 239–365, 1988.
49. ZAPROWSKI, B.; PAZZAGLIA, F.; EVENSON, E. Climatic influences on profile concavity and river incision, **Journal of Geophysical Research**, electronic edition, v. 110, n. F3, doi:10.1029/2004JF000138, 2005.

Manuscrito recebido em: 14 de Maio de 2014
Revisado e Aceito em: 04 de Dezembro de 2014